Validation of a bulk turbulence model with thermal images of a point source

Gerard J. Kunz, Marcel M. Moerman, Peter J. Fritz and Gerrit de Leeuw

TNO-Physics and Electronics Laboratory
P.O. Box 96 86 4, 2509 JG The Hague, The Netherlands
Tel. +31 70 374 04 60   Fax +31 70 328 09 61   E-mail: kunz@fel.tno.nl

ABSTRACT

A model was developed for the prediction of turbulence in the marine surface layer. The model requires standard meteorological values of air temperature, air humidity, wind speed each from any given height from within the surface layer and the sea surface temperature. Internally, the model is controlled by the exchange coefficients for momentum, heat and water vapor. A variant using the surface roughness length in stead of the drag coefficient has also been implemented. The micrometeorological output parameters of the model are used to predict vertical profiles of the refractive index -to predict refractivity effects- and profiles of the refractive index structure function parameter $C_n^2(z)$. The latter is the controlling parameters to calculate optical turbulence effects such as scintillation and blurring. Experimental data were obtained from images taken of a point source over a 19 km path over the North Sea at a frame rate of 25 Hz using a 3-5 μm infrared camera system. The images were analyzed for scintillation, blur and image dancing. Predicted and measured turbulence effects are compared.

Keywords: turbulence, micrometeorological model, optical turbulence, infrared

1. INTRODUCTION

High quality, long range imaging, requires state of the art optical systems which combine high resolution and high sensitivity. However, under operational conditions, the performance of these systems can seriously be degraded due to atmospheric effects such transmission losses, contrast reduction, refraction and turbulence. Effects due to transmission losses and/or contrast reduction can partly be compensated using contrast enhancing techniques and/or signal averaging. Correction for atmospheric refraction and turbulence is difficult if possible. In stead, scenarios in technical decision aids can be modified if the circumstances under which this occurs can be recognized. Atmospheric refractive effects such as sub- and super-refraction are caused by typical vertical distributions of the refractive index which can be calculated from the vertical distribution of air temperature, humidity and pressure using standard expressions. Optical turbulence is closely related to variations of the refractive index in time and space. Thus knowing the variations of temperature, humidity and pressure, effects of optical turbulence can be estimated. These variations can be derived from expressions available in micrometeorology commonly used to predict the vertical profiles of wind speed, temperature and humidity in addition to the fluxes of momentum, heat and water vapor. Using standard meteorological observations of wind speed, air temperature and humidity at the given height in combination with the sea surface temperature, the set of micrometeorological equations can be solved and the basic turbulent parameters to predict optical turbulence are obtained. An experiment was carried out to predicted turbulent effects based on standard meteorological observations. A concise description of the model, illustrated with some model calculations, is given in section 2. A short description of the field experiment with some initial results is given in section 3. A comparison of the model calculations and the experimental data is presented in section 4.

2 TURBULENCE MODEL

In micrometeorology equations are available to predict the vertical profiles of wind speed, temperature and humidity. These equations use the friction velocity, scaling temperature, scaling humidity, roughness lengths and a parameter describing the atmospheric stability which is in turn a function of the before mentioned parameters. A solution of the set of

equations requires a reference wind speed, temperature and humidity at a certain -but not necessarily the same- height and the sea surface temperature. Internally, the model uses empirical values for the exchange coefficients for the fluxes of momentum, heat and water vapor which are also used in the process to calculate the friction velocity, scaling temperature, scaling humidity and the roughness lengths. Nevertheless, the large number of equations involved form a closed set of implicit equations which can be solved iteratively. The profile of air pressure can separately be calculated using the hydrostatic equation. The basic equations for the micrometeorological model[1,2,3,4] have been used to develop a model that requires only standard meteorological observations from any given height and the sea surface temperature. Internally, the model uses fixed values for the 10 m neutral exchange coefficients for heat and water vapor flux and a wind speed dependent neutral drag coefficient for momentum flux. Empirical values of these parameters are available from literature. Roughness lengths for wind speed, temperature and humidity are evaluated separately in the model. Internal tests of the model show that the reproduction of the input condition, using the calculated output parameters, is better than 10^{-8}. The overall performance of the model -based on the roughness length for wind speed- is in excellent agreement with the only available data set in open literature[5].

After having solved the set of micrometeorological equations the vertical profile of refractive index can be calculated from the profiles of air temperature, pressure and humidity[6]. Figure 1 shows the refractivity N= (n-1).10^6 at sea level for 0.55 μm as a function of air temperature and humidity. The absolute value of the refractivity at 10 μm is different but that the variation with temperature and humidity are very much alike. A few examples of the vertical profile of the refractivity are presented in Figure 2. Again, the absolute values of the refractivity for the two wavelengths differ in absolute sense but the shape of the profiles are similar. This means that refractive effects for the two optical wavelengths will also be similar.
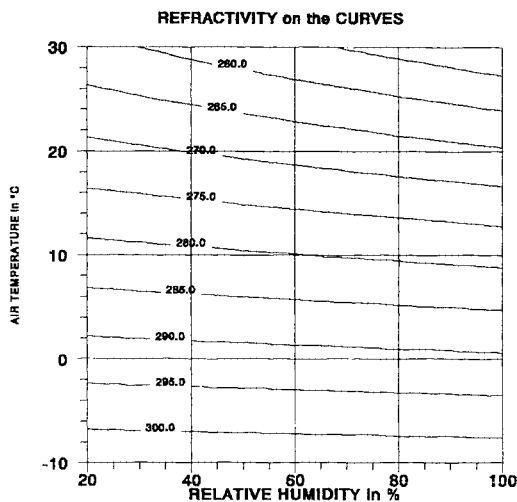

Figure 1: Calculated refractivity N as a function of air temperature and relative humidity
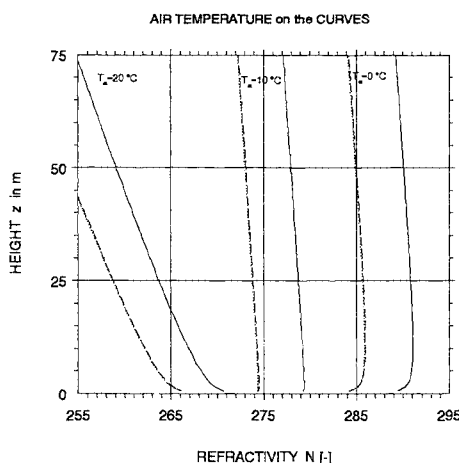

Figure 2: Vertical profiles of the refractivity for 10 μm (solid lines) and for 0.55 μm (dashed lines).at three different air temperatures. The results were calculated for U= 10 m/s, RH= 80 %, T_{sea}= 10 °C and P= 1025 hPa.

The refractive index structure function parameter C_n^2, which is the driving parameter for describing turbulence effects, is calculated from the structure function parameters for temperature and humidity and the covariance between the two in combination with the variability of the refractive index with temperature and humidity. The refractive index structure function parameter is calculated using (1).

$$C_n^2 = \left(\frac{\partial n}{\partial T}\right)^2 C_T^2 + \left(\frac{\partial n}{\partial q}\right)^2 C_q^2 + 2\left(\frac{\partial n}{\partial T}\frac{\partial n}{\partial q}\right) C_{Tq} \tag{1}$$

The variability of the refractive index with temperature and humidity is shown in Figure 1. The values of C_T^2 and C_q^2 are calculated using:

$$C_T^2 = z^{-2/3} T_*^2 f_1(z/L) \tag{2a}$$

$$C_{Tq} = z^{-2/3} T_* q_* f_2(z/L) \tag{2b}$$

$$C_q^2 = z^{-2/3} q_*^2 f_3(z/L) \tag{2c}$$

Expressions for the empirical functions f_1, f_2 and f_3 can be found in literature[7,8,9,10,11,12,13,14,15]. The scaling temperature T_* and the scaling humidity q_* are provided by the meteorological model as well as the Monin-Obukhov length L. The parameter z is the height above the surface. Calculated values of the refractive index structure function parameter are shown as contour lines in Figure 3 as a function of air-sea temperature difference (ASTD) and wind speed. These data are for an altitude of 10 m above the surface and are for the optical wavelengths of both 10 µm and 0.55 µm.
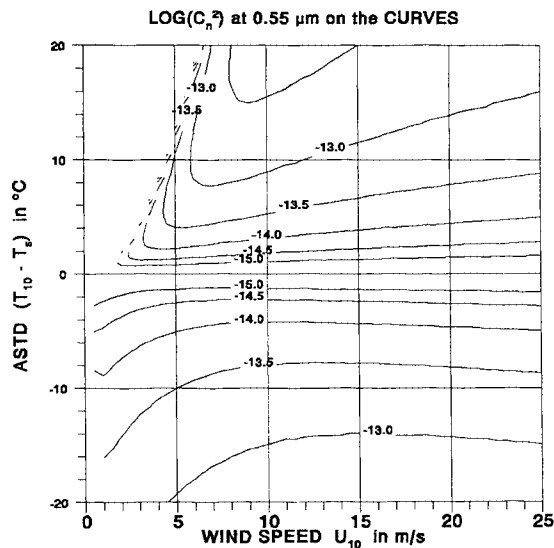

LOG(C_n^2) at 0.55 µm on the CURVES

Figure 3: Contour lines of the refractive index structure function parameter -log values are on the curves- as a function of the ASTD and wind speed. The model calculations based on a wind speed dependent neutral drag coefficient. The presented results are valid for both 10 µm and 0.55 µm wavelengths.

The explicit dependence of the refractive index structure function parameter on wind speed and ASTD are presented in Figure 4a+b.
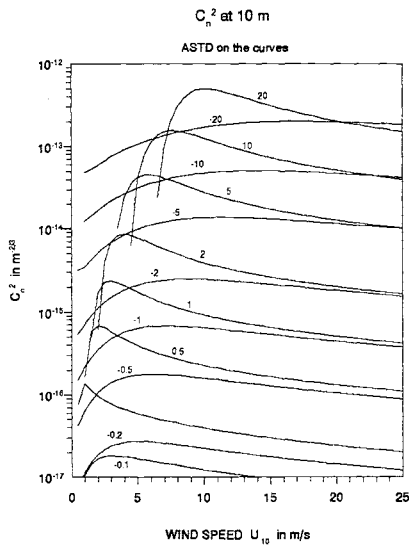
C_n^2 at 10 m

ASTD on the curves

C_n^2 at 10 m

WIND SPEED in m/s on the CURVES

Figure 4a: Refractive index structure function parameter for 10 μm and 0.55 μm wavelengths as a function of 10 m wind speed for different values of the ASTD. The results are based on a wind speed dependent neutral drag coefficient.
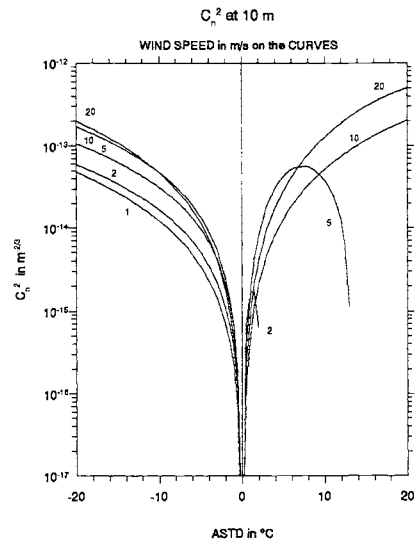
Figure 4b: Refractive index structure function parameter for 10 μm and 0.55 μm wavelengths as a function of 10 m ASTD for different values of the wind speed. The results are based on a wind speed dependent neutral drag coefficient.

Vertical profiles of the refractive index structure function parameter are presented in Figure 5. These data ware calculated for different values of the ASTD and for a fixed wind speed of 10 m/s. The results are valid for both 10 μm and 0.55 μm wavelengths. The steepest curves are for negative values of the ASTD -unstable situations-. Note that the strongest gradients take place in about the lowest 10 m.

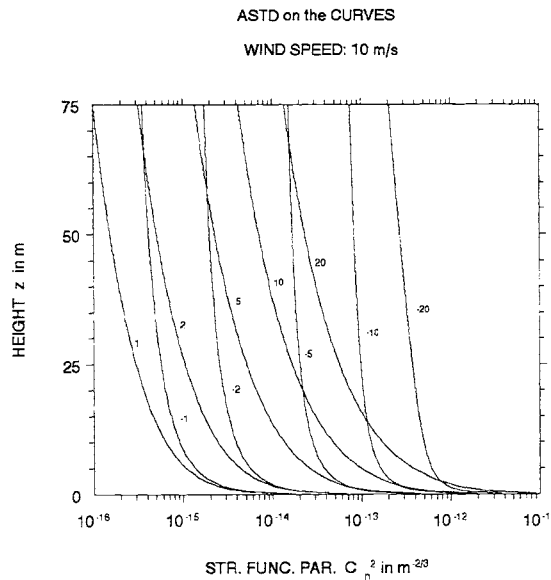ASTD on the CURVES

WIND SPEED: 10 m/s

Figure 5: Vertical profiles of the refractive index structure function parameter for 10 μm and 0.55 μm for different values of the ASTD and a fixed wind speed of 10 m/s.

Scintillation is assumed to be caused by the randomly variable, normally distributed, real part of the propagation constant, σ_χ. The Rytov approximation[16,17,18,19] for spherical waves predicts a relation between σ_χ and the structure constant for the refractive index C_n^2 over a non homogeneous path R according to:

$$\sigma_\chi^2(R) = 0.56 \left(\frac{2\pi}{\lambda}\right)^{7/6} \int_0^R C_n^2(r) \left(\frac{r}{R}\right)^{5/6} (R-r)^{5/6} \, dr \tag{3}$$

Rytov's approximation is based on weak turbulence only[18,20]. Therefore, equation (3) does not predict the saturation of σ_χ^2 at a value of about 0.3 ($\sigma_\chi > 0.55$) which is observed experimentally.

Scintillation is described in terms of a Gaussian distributed electromagnetic propagation constant with standard deviation σ_χ. As a result, the intensity variations are log-normally distributed and the relation between the mean intensity and the standard deviation[18,20,21] is given by:

$$\frac{\sigma_I^2}{\bar{I}^2} = e^{4\sigma_\chi^2} - 1 \tag{4}$$

Due to the saturation[18,20] the ratio of the standard deviation and the mean intensity saturates at about 1.1. Calculated values for the scintillation as a function of wind speed and ASTD for 10 km path length and for 0.55 μm are presented in Figure 6a.

Blur, image dancing and deformation are described in terms of the transversal coherence length ρ_o. The transversal coherence length can be regarded as the maximum diameter of the optics before the effects of turbulence distort the image. It is defined as[18]:

$$\rho_o = \left[1.46 \left(\frac{2\pi}{\lambda}\right)^2 \int_0^R C_n^2(r) \, (r/R)^{5/3} \, dr \right]^{-3/5} \tag{5}$$

The atmospheric Modulation Transfer Function (MTF), expressed in cycles per unit length, is derived using the atmospheric coherence length (see equation 8). For long term exposures[18] the MTF for a system with focal length f is given by:

$$MTF(\upsilon) = \exp[-3.44 \, (\lambda f \, v/r_o)^{5/3}] \tag{6}$$

and for short term exposure the MTF is calculated according to:

$$MTF(\upsilon) = \exp\{-3.44 \, (\lambda f \, v/r_o)^{5/3} [1 - b(\lambda f \, \upsilon/D)^{1/3}]\} \tag{7}$$

where the atmospheric coherence length r_o is directly derived from the transversal coherence length ρ_o according to:

$$r_o = 2.1\rho_o \tag{8}$$

For our (far field) applications, the constant b in the equation is taken to be 0.5 (see ref. 18). Equation (7) shows that for short term exposure, the atmospheric turbulence cannot be treated independently from the system.

The blur size has been approximated by considering that one line pair in the focal plane can be represented by an angle of $1/fv$ (radians) and that the influence of turbulence becomes only noticeable under conditions were r_o becomes so small that the numerical value of the exponent in equation (7) reduces to -1. The size of the calculated blur is presented in Figure 6b as a function of wind speed and ASTD. It was noted that the blur in the IR is about a factor of two smaller than in the visible. The results in Figure 6b show that the blur is strongly dependent on the ASTD and weakly dependent on the wind speed.
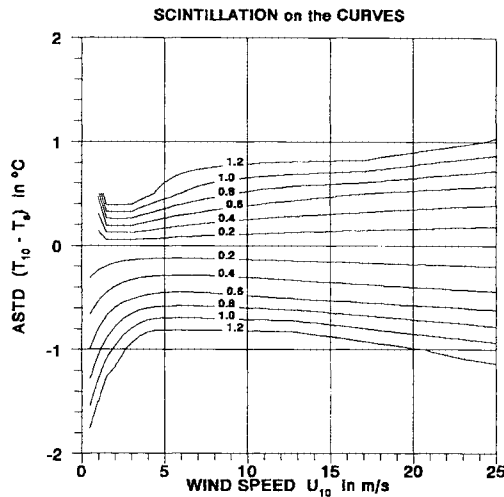

Figure 6a: Contour lines of the calculated scintillation as a function of wind speed and ASTD for 10 µm over a 10 km path at 10 m above the surface.
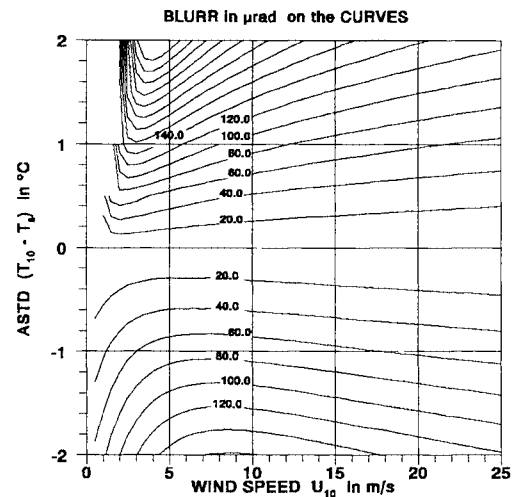
Figure 6b: Contour lines of the calculated blur as a function of wind speed and ASTD for 10 µm over a 10 km path at 10 m above the surface.

Image motion is expressed as the variation around a mean value of the angle of arrival of the wave[20]. The variance of the angle of arrival can be expressed as:

$$< \alpha_x^2 > \quad = \quad < \alpha_y^2 > \quad \cong \quad 4.5\, f^2\, a^{-1/3} \int_0^R C_n^2(r)\, dr \tag{9}$$

Although image motion cannot be decoupled from the system parameters, we can make an estimate of the angles of arrival under isotropic turbulence from the data. For a system with a focal length of 1 m, an aperture diameter of 0.2 m and a range of 10 km, the angle of arrival becomes about 77,000 times the refractive index structure function parameter. Thus for weak turbulence with $C_n^2 = 10^{-17}$ m$^{-2/3}$, the angle of arrival becomes about 10^{-12} radians and for strong turbulence with $C_n^2 = 10^{-12}$ m$^{-2/3}$, the angle of arrival becomes about 10^{-7} radians which is within the blur circle of the system described in section 3.

3 EXPERIMENT

Effects of atmospheric turbulence in the marine surface layer were experimentally studied using a point source and a Cincinnati IRC-64 infrared (3-5 µm) camera system. The camera with reflecting telescope (D = 30 cm, f = 1 m) were placed on a tower of the Pier of Scheveningen, about 400 m of the coast, about 40 m above the water surface. The point source, a 70 cm parabolic reflector with a heated tungsten element in the focal plane, was mounted to Meetpost Noordwijk at about 10 m above the mean water surface. Meetpost Noordwijk is a stable platform in the North Sea at about 9 km off the Dutch coast and about 19 km from the Pier of Scheveningen. The camera operated with a frame rate of 25 Hz. Bursts of 250 images

were recorded with the parameters of the actual meteorological conditions. About 300 bursts were recorded over a period of 6 months under different weather conditions. The images were analyzed for peak intensity, integrated intensity over the imaged point source, an effective diameter of the image, the ellepticity and both the horizontal and the vertical skewness and kurtosis.

One example of a time series of the peak power, integrated power over the point image (both in arbitrary units) and the spot size (expressed in pixel size) are presented in Figure 7. These data were measured on a clear day with a wind speed of 8.2 m/s and a positive value of the ASTD of 8.1 °C. A scatter plot with the spot size, the integrated power over the spot size both and the peak intensity on the axes is presented in Figure 8.
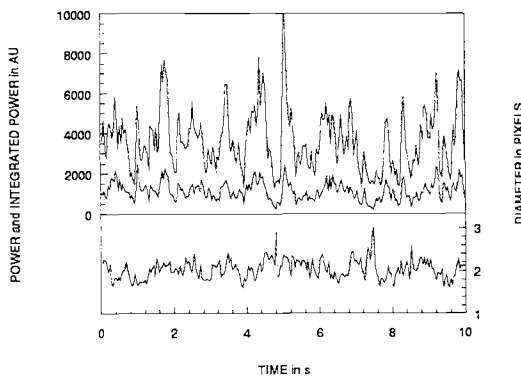
Figure 7: Upper figure: the variation of integrated power (upper of the two curves) and the peak power (lower of the two curves) as a function of time. Lower figure: the size of the point image, expressed in pixel size (50 μm) of the camera. Data recorded on May 12, 1994 at 2:54 pm.
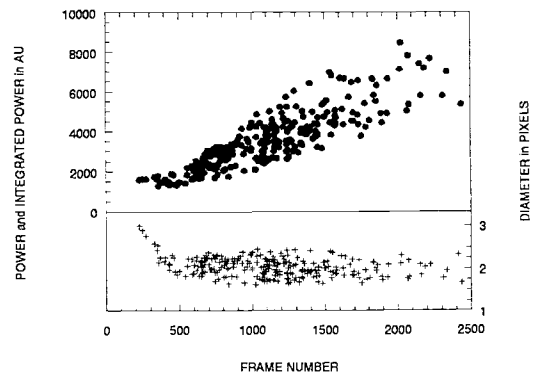
Figure 8: Scatter plot of the integrated power of the point image and the spot size as a function of the peak power.

4 COMPARISON

To eliminate influences of the coastal area, data recorded during periods of on shore wind were selected for further analysis. The mean values and the standard deviations of the peak power, integrated power and spot size were used to calculate the experimental values of scintillation, blurring and refractive index structure function parameters. These parameters were compared with the predicted data from the model that is driven by the meteorological condition. Scatter plots of the scintillation and blur are presented in Figure 9 and 10. The relation between the modeled and measured values of the refractive index structure function parameter is shown in Figure 11.
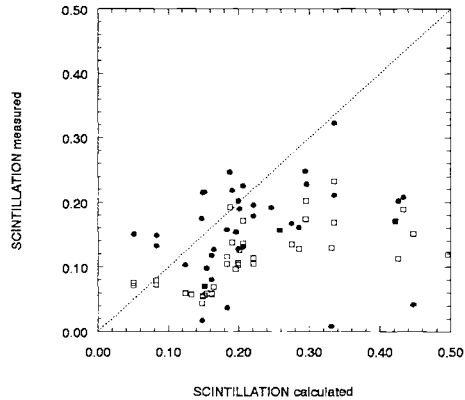
Figure 9: Scatter plot of the measured scintillation and the modeled scintillation. Solid dots are based on peak power. Open squares are based on integrated power over the imaged point source.
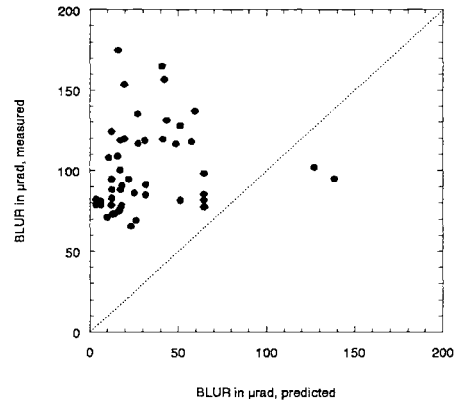

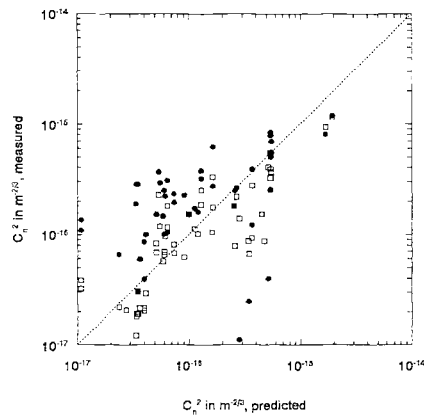Figure 10: Scatter plot of the measured blur and modeled blur. Pixel size is 50 μrad.

Figure 11: Scatter plot of the measured and modeled refractive index structure function parameter.

5 CONCLUSION

A model was developed to predict turbulence in the marine surface layer and the vertical profiles of wind speed, temperature and humidity. The input parameters for the model are wind speed, air temperature, humidity and pressure from any given height within the surface layer and the sea surface temperature. The results are used to calculate profiles of the refractive index and the refractive index structure function parameter for the prediction of respectively refractivity effects and optical turbulence. The performance of the model is in excellent agreement with results available from literature. Experimental data were obtained with a point source and an IR camera over a 19 km path over the sea in a coastal area. The first results of the analysis indicate that the measured and modeled turbulence effects (refractive index structure function parameters and scintillation) are in reasonable agreement. As expected, the experimental data obtained during off shore winds did not match the predicted values of the model.

6 REFERENCES

1. Tennekes, H. and J.L. Lumley, "*A first course in turbulence*," The MIT Press, Cambridge, Massachusetts, and London, England, ISBN 0 262 200198, 1972.
2. Businger, J., "*Turbulent transfer in the atmospheric surface layer*," in 'Workshop on Micrometeorology', edited by D.A. Haugen, American Meteorological Society, Boston, Library of Congress 73-80936, 1973.
3. Panofski, H.A. and J.A. Dutton, "*Atmospheric turbulence: models and methods* for engineering *applications*," John Wiley & Sons, New York, USA, ISBN 0 471 05714 2, 1984.
4. Stull, R.B., "An introduction to boundary layer meteorology," Kluwer Academic Publishers, Dordrecht, Boston, London, ISBN 90 277 2768-6, 1988.
5. Smith S.D., "Coefficients for sea surface wind stress, heat flux, and wind profiles as a function of wind speed and temperature," *J. Geophys. Res., 93*, 15,467-15,472, 1988.
6. Edlén, B., 'The refractive index of air', *Meteorology*, 2, 71-80, 1966.
7. Fairall, C.W., G.E. Schacher, and K.L. Davidson, "Measurements of the humidity structure function parameters C_q^2 and C_{Tq} over the ocean," *Bound-Layer Meteor., 19*, 81-92, 1980.
8. Davidson, K.L., T.M. Houlihan, C.W. Fairall and G.E. Schacher, "Observation of the temperature structure function parameter, C_t^2 over the ocean," *Bound. -Layer Meteor., 15*, 507-523, 1978.
9. Davidson, K.L., G.E. Schacher, C.W. Fairall, and A.K. Goroch, "Verification of the bulk method for calculating over water optical turbulence," *Appl. Opt., 20*, 2919-2924, 1981.
10. Kunkel, K.E., and D.L. Walters, "Modeling the diurnal dependence of the optical refractive index structure parameter," *J. Geophys. Res., 88*, 10.999-11.004, 1983.
11. Fairall, C.W., and S.E. Larsen, "Inertial dissipation methods and turbulent fluxes at the air ocean interface," *Bound.-Layer Meteor. 34*, 287-301, 1986.
12. Hill, R.J., "Structure functions and spectra of scalar quantities in the inertial-convective and viscous-convective ranges of turbulence," *J. Atm. Sci., 46*, 2245-2251, 1989.
13. Thiermann, V., and A. Kohnle, "Modeling of optically and IR effective atmospheric turbulence," in *Atmospheric Propagation in the UV, Visible and IR and mm-wave region and related systems aspects*, pp. 19.1-19.12, Proc. AGARD Symposium No. 44 Copenhagen, Denmark, 1989.
14. Hill, R.J., and G.R. Ochs, "Surface-layer similarity of the temperature structure parameter," *J. Atm. Sci., 49*,1348-1353, 1992.
15. Hill, R.J., G.R. Ochs, and J.J. Wilson, "Measuring surface-layer fluxes of heat and momentum using optical scintillation," *Bound-Layer Meteor., 58*, 391-408, 1992.
16. Andreas, E.L., Selected papers on turbulence in a refractive medium, *SPIE Milestones Series, Vol. 25*, Soc. of Photo-Optical Instrumentation Engineers, Bellingham, WA, USA, 1990.
17. Beland, R.R., E.A. Murphy, G.G. Koenig, and P.C. Thomas, "Comparison of horizontal scintillation measurements and models", in *Optical, Infrared and Millimeter Wave Propagation Engineering, SPIE Proc. 926*, 44-51, 1988.
18 Beland, R.R., "Propagation through Atmospheric Optical Turbulence," in *The Infrared & Electro-Optical Systems Handbook: Atmospheric Propagation of Radiation* vol. 2, edited by F.G. Smith, pp. 157-232, Infrared Information Analysis Center, Ann Arbor, Michigan 48113-4001 and SPIE Optical Engineering Press, Bellingham, WA, USA, 1993.
19. Ochs, G.R., and T. Wang, "Finite aperture scintillometer for profiling wind and C_n^2," *Appl. Opt. 17*, 3774-3778, 1978.
20. Hufnagel, R.F., "Propagation through Atmospheric Turbulence," in *The Infrared Handbook*, edited by W.L. Wolfe and G.J. Zissis, pp. 6.1-6.56, Office of Naval Research, Dept. of the Navy, Washington, DC, 1978.
21. Goodman, J.W. *Statistical Optics*, Wiley, New York, 1985.